

Formation of silicon oxide grains at low temperature

S. A. Krasnokutski, G. Rouillé, C. Jäger, F. Huisken

Laboratory Astrophysics Group of the Max Planck Institute for Astronomy at the Friedrich Schiller University Jena, Institute of Solid State Physics, Helmholtzweg 3, D-07743 Jena, Germany

Sergiy.Krasnokutskiy@uni-jena.de

S. Zhukovska, Th. Henning

Max Planck Institute for Astronomy, Königstuhl 17, D-69117 Heidelberg, Germany

ABSTRACT

The formation of grains in the interstellar medium, i.e., at low temperature, has been proposed as a possibility to solve the lifetime problem of cosmic dust. This process lacks a firm experimental basis, which is the goal of this study. We have investigated the condensation of SiO molecules at low temperature using neon matrix and helium droplet isolation techniques. The energies of SiO polymerization reactions have been determined experimentally with a calorimetric method and theoretically with calculations based on the density functional theory. The combined experimental and theoretical values have revealed the formation of cyclic $(\text{SiO})_k$ ($k = 2-3$) clusters inside helium droplets at $T = 0.37$ K. Therefore, the oligomerization of SiO molecules is found to be barrierless and is expected to be fast in the low-temperature environment of the interstellar medium on the surface of dust grains. The incorporation of numerous SiO molecules in helium droplets leads to the formation of nanoscale amorphous SiO grains. Similarly, the annealing and evaporation of SiO-doped Ne matrices lead to the formation of solid amorphous SiO on the substrate. The structure and composition of the grains were determined by infrared absorption spectroscopy, transmission electron microscopy, and energy-dispersive X-ray spectroscopy. Our results support the hypothesis that interstellar silicates can be formed in the low temperature regions of the interstellar medium by accretion through barrierless reactions.

Subject headings: ISM: dust formation — ISM: silicate dust — low-temperature chemistry

1. INTRODUCTION

Stars used to be seen as both the origin and the sinks of cosmic dust grains. Indeed grains are formed in the shell of AGB stars and supernovae. This so-called stardust is expelled from the stellar environments, dispersed in the interstellar medium (ISM), and eventually consumed by star formation processes. These processes limit the lifetime of cosmic dust grains in the ISM to $\sim 2 \times 10^9$ yr (Draine 2009). If one takes additional destructive mechanisms into account, e.g., shattering and sputtering in interstellar shocks, their lifetime is further reduced to $\sim 4 \times 10^8$ yr (Barlow & Silk 1977; Draine & Salpeter 1979;

Jones et al. 1994). This value, however, is not consistent with the timescale of dust injection by stars of 3×10^9 yr in the ISM. It was recently estimated that only a few percent of the total mass of the dust in the ISM is stardust (Zhukovska et al. 2008; Draine 2009). This discrepancy was first noted by Draine & Salpeter (1979) and later confirmed by several other studies (e.g., Dwek & Scalo 1980; Weingartner & Draine 1999). It suggests that an intensive growth of dust particles actually takes place directly in the ISM. At the present time it is assumed that most of the material in interstellar dust grains was formed in the ISM (Weingartner & Draine 1999; Draine 2009). However, Jones & Nuth (2010) have reconsidered the

discrepancy between dust destruction and formation processes in the ISM and found that based on inherent uncertainties there could be a compatible injection and destruction time scale of silicate dust. They also noted that the spectra of grains where metals had been plated out on the surface could be different from the spectra of silicates observed in the ISM.

Silicates are the main components of interstellar dust (Henning 2010). The conditions for the silicate growth in the ISM are presently not known. We assume that the grain growth occurs in dark, dense molecular clouds at temperatures between 10 and 20 K (Herbst 2001). Consequently, we intend to study the formation of silicates at cryogenic temperatures. As a first step of our project, we have carried out experiments on the condensation of SiO molecules. The formation of $(\text{SiO})_k$ ($k = 2-4$) oligomers by aggregation of SiO molecules was already found to proceed at low temperatures, by means of laboratory experiments (Anderson et al. 1968; Hastie et al. 1969; Anderson & Ogden 1969; Khanna et al. 1981). In addition, quantum chemical calculations also predicted the barrierless oligomerization reaction (Lu et al. 2003; Avramov et al. 2005). In contrast, Pimentel et al. (2006) determined an energy barrier of 8 kcal mol⁻¹ for the reaction between Si₂O₂ and SiO. Beside this initial stage of cluster formation, first indications of the formation of solid magnesium silicates were also observed when a nitrogen matrix containing isolated SiO molecules and Mg atoms was evaporated. The deposit produced in this way showed absorption bands at 10 and 20 μm , which were very similar to interstellar absorption features (Donn et al. 1981).

In this work, we extend these studies by addressing the question of energy barriers in the cluster formation processes and by evaluating the binding energy of the clusters. Experiments have been carried out in superfluid helium droplets at 0.37 K and in neon matrices at 6–11 K. They were completed with theoretical calculations. Finally, we have analyzed the structure of grains formed at low temperature in our experiments. We show that there is no barrier for the aggregation of SiO molecules and that the grains formed in our experiments are actually SiO grains with an amorphous structure and a reactive surface.

2. EXPERIMENTAL AND COMPUTATIONAL DETAILS

2.1. Matrix Isolation Spectroscopy

The matrix isolation technique is a common method to study chemical reactions at low temperatures and has been the subject of different reviews (e.g., Jacox 2002; Andrews 2004). The matrix isolation spectroscopy apparatus used in the present experiment was extensively described in a previous publication (Rouillé et al. 2012). Briefly, it consists of a commercial UV/VIS spectrometer (JASCO V-670 EX) coupled to a vacuum chamber by means of optical fibers. The chamber is equipped with a closed-cycle He cryocooler (Advanced Research Systems Inc. DE-204SL). We used Ne (Linde, purity 99.995%) as the matrix material. During the course of each experiment, a CaF₂ substrate was placed into the vacuum chamber and cooled to a temperature of 6 K by the action of the cryocooler. Silicon monoxide molecules were prepared by laser vaporization applied to silicon monoxide powder (Sigma-Aldrich) pressed into a pellet. The fourth harmonic ($\lambda = 266$ nm) of a pulsed ($f = 10$ Hz) Nd:YAG laser was used for this purpose. Laser pulses of 1.5 mJ energy and 5 ns duration were focused to a spot of about 0.45 mm in diameter at the surface of the pellet. The evaporated molecules were co-condensed onto the cold substrate with the rare gas, which was fed into the vacuum chamber at a flow rate of 7 sccm (standard cubic centimeter per minute).

2.2. Helium Droplet Experiments

In spite of the many advantages provided by conventional solid rare gas matrices, it has a serious limitation as the mobility of the species trapped is considerably reduced. In contrast, liquid helium droplets provide an ultralow temperature of $T = 0.37$ K and are proven to be superfluid (Hartmann et al. 1996b). Therefore, all species embedded inside the He droplets are allowed to move freely, thus resembling the situation in the gas phase. As a result, helium droplets provide an ideal possibility to study chemical reactions and aggregations at low temperature. The doping of single helium droplets with several species allows to study the condensation of the embedded species. The formation of van der Waals clusters (Hartmann et al. 1996a) and metal

nanoparticles (Loginov et al. 2011a) was demonstrated to occur inside the helium droplets. Alternatively, the chemical reactions between embedded species can be studied at ultralow temperature. The absence of an entrance channel barrier for several chemical reactions was demonstrated (Krasnokutski & Huisken 2010a,b, 2011). In particular, the barrierless oxidation of silicon atoms and clusters by oxygen molecules was found (Krasnokutski & Huisken 2010a).

The He droplet apparatus is basically the same as that reported earlier (Krasnokutski et al. 2005). It consists of three differentially pumped chambers. In the source chamber, large helium clusters are produced by supersonic expansion of pure helium gas at high pressure ($p = 20$ bar) through a $5 \mu\text{m}$ diameter pinhole nozzle, cooled by liquid helium. The average number of He atoms (N_{He}) per droplet is evaluated according to the empirical relation

$$N_{\text{He}} = 852393.161 \exp(-0.3591 T), \quad (1)$$

where T is the temperature of the nozzle in K. This equation has been derived by fitting the experimental data of Toennies & Vilesov (2004). In the second chamber, the He droplets are doped with foreign species. The doping occurs by collision of the helium droplets with gas phase atoms or molecules. Upon the collisions, the gas phase species are picked up by the helium nanodroplets and carried by them to the third chamber. This chamber contains a quadrupole mass spectrometer detector equipped with an electron bombardment ionizer.

Alternatively, an appropriate substrate can be placed into the helium droplet beam. In this case, after the collision of the helium droplets with the substrate, the liquid helium is evaporated, leaving the condensable content of the droplets on the substrate. After removal of the substrate from the vacuum chamber, the deposited material can be analyzed by high-resolution transmission electron microscopy (HRTEM) and energy-dispersive X-ray spectroscopy (EDX).

We performed four experiments using different precursor combinations (1. Si and H_2O molecules; 2. SiO molecules; 3. SiO and H_2O molecules; 4. SiO, H_2O , and O_2 molecules) in helium droplets. For the incorporation of Si atoms, commercially available silicon wafer (CrysTec) was evaporated

(for details, see Krasnokutski & Huisken 2010a). In experiments with SiO molecules, a sample of silicon monoxide (SiO) or synthetic quartz (SiO_2) powder was heated in a zirconia crucible surrounded by a water-cooled jacket. In both cases, SiO molecules are the main species released into the gas phase. In case of the SiO_2 evaporation, additional oxygen is produced. Silicon monoxide was used to study the initial cluster formation by mass spectrometry while quartz was employed to condense nanoscale grains. The vapor pressure of SiO decreases with increasing evaporation time because of a structural modification of the original SiO powder. The vapor pressure of SiO obtained by heating quartz powder is more stable, but requires a higher evaporation temperature. Thus silicon monoxide powder is more suitable as a precursor for the fast mass spectrometry measurements while quartz powder is chosen for the more time-consuming study of grain condensation. Finally, it is not necessary to use a dedicated source to incorporate H_2O molecules in He droplets as H_2O is present in every standard vacuum apparatus as residual gas. In studies involving water molecules, the residual gas pressure was adjusted to a stable value of approximately 4×10^{-6} mbar. When the incorporation of water was not desired, the concentration of water molecules was reduced by filling a cold trap with liquid nitrogen, which resulted in an improvement of the pressure to about 3×10^{-7} mbar. At this condition, only a minor amount of helium droplets (less than 3 %) picked up the water molecules. Due to the geometry of the apparatus, the pickup of water molecules occurs after that of the Si or SiO species. The concentration of water and other impurities was monitored by quadrupole mass spectrometer analyses. The incorporation of other impurities into the He droplets could not be detected.

2.3. Theoretical calculations

Molecular geometries of $(\text{SiO})_k$ clusters were determined using the B3LYP/6-311+G** and CCSD(T)/cc-pVTZ levels of theory implemented in the GAUSSIAN09 software package (Frisch et al. 2009). The reaction energies were obtained as the difference between the electronic and zero point energies of the reactant and product molecules. CCSD(T)/cc-pVTZ quantum chemical calculations provide high levels of accuracy of about 20 kJ

mol^{-1} for the reaction energy (Delley 2006).

3. RESULTS

3.1. Matrix Isolation Study

The laser-evaporated SiO molecules were co-condensed with the Ne gas on the CaF_2 substrate at 6 K. The UV spectrum of this matrix is displayed in Figure 1. The vibrational progression of the $A^1\Pi \leftarrow X^1\Sigma^+$ transition of SiO was previously observed in other inert matrices (Shirk & Bass 1968; Hormes et al. 1983) and can be easily identified in our spectrum where it spreads from 235 nm towards shorter wavelengths. In addition, one observes a broad band at 240 nm and two structured features at 280 and 320 nm. Then, we increased the temperature of the substrate several times to $T = 10\text{--}11$ K. At these temperatures, the Ne matrix slowly starts to sublime. Additionally, all isolated species gain some partial mobility inside the matrix, which allows these species to aggregate and form clusters. As can be seen in Figure 1, after an annealing at 10 and 11 K, the intensity of the SiO bands was noticeably reduced. This is due to the aggregation of isolated SiO molecules and the formation of some

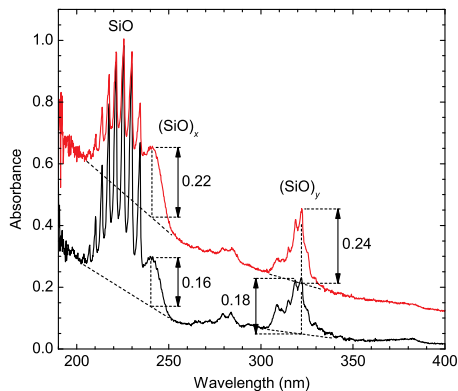


Fig. 1.— Electronic spectra of single SiO molecules and their oligomers isolated in a Ne matrix at $T = 6$ K. The lower (black) spectrum was obtained directly after co-deposition of the laser-evaporated SiO molecules and the matrix gas. The upper (red) spectrum shows the result of an annealing of the matrix for 15 min at $T = 10$ K and 10 min at $T = 11$ K. (A color version of this figure is available in the online journal.)

larger clusters. At the same time, the absorption features at 240 and 320 nm increased in intensity. Therefore, these bands are likely due to $(\text{SiO})_k$ clusters. This assignment is also supported by the fact that, in previous studies, $(\text{SiO})_2$ and $(\text{SiO})_3$ molecules were present in the matrices together with SiO and that the intensity of the absorption bands assigned to these molecules rose upon annealing of the matrix (Friesen et al. 1999, and references therein). Moreover, the absorption features of these molecules were predicted to be in the range between 200 and 400 nm (Reber et al. 2008; Xu et al. 2010). Our results are in line with the previous studies of SiO aggregation at low temperatures, which demonstrated the formation of small $(\text{SiO})_k$ ($k = 2\text{--}4$) clusters using different experimental techniques (Hastie et al. 1969; Anderson & Ogden 1969; Khanna et al. 1981; Schnöckel et al. 1989; Friesen et al. 1999; Pimentel et al. 2006).

After having taken the spectra of Figure 1, the temperature of the matrix was slowly raised, allowing the matrix to evaporate completely. After the evaporation of the matrix, a solid condensate remained on the substrate. In situ UV spectra measurements, taken at room temperature while the substrate was still under vacuum, have demonstrated that the extinction caused by the condensate was characterized by a smooth curve rising towards shorter wavelengths. Therefore, the observed extinction can be attributed to scattering caused by the grains. Their analysis by EDX revealed a Si/O ratio of about 1. Transmission electron microscopy (TEM) images of the particles are shown in Figure 2. All observed particles have an amorphous structure with the size of the smallest grains being around several tens of nanometers. The smaller particles form larger aggregates of micrometer size.

A single grain of about $20 \mu\text{m}$ in diameter was selected from the condensate to measure its infrared (IR) absorption spectrum in a range between 600 and 4000 cm^{-1} using an IR microscope. The spectrum is shown in Figure 3. Absorption peaks are observed at $751, 843, 873, 932, 1052, 1164, 1614, 2159, 2248,$ and 3327 cm^{-1} . The strong bands at 1052 and 1164 cm^{-1} are assigned to the transverse and longitudinal modes of the Si–O–Si asymmetric stretching vibrations commonly observed in SiO_2 . For the purpose of compari-

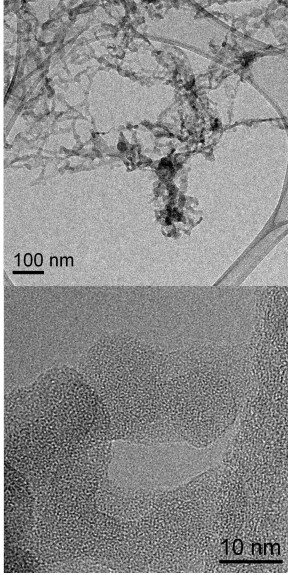


Fig. 2.— TEM images showing the condensate collected after the annealing and evaporation of a Ne matrix doped with SiO molecules and oligomers.

son, a spectrum of amorphous SiO₂ produced by the sol gel technique was added to Figure 3. The strong similarity of the broad 10 μm band with the band of a SiO₂ material point to a certain stoichiometric separation and disproportionation of the SiO into silicon and silica. Recent experimental studies on the structure and chemical composition of solid SiO clearly confirm the inhomogeneity of solid SiO in a nanometer- or subnanometer scale. The formation of phases consisting of Si and SiO₂ and the formation of the typical SiO₄ groups connected by oxygen bridges in addition to Si-Si groups have been proven by different authors (Ferguson & Nuth 2012; Hohl et al. 2003). In addition, quantum chemical computations comparably demonstrate the tendency of SiO clusters to form SiO₄ in addition to Si-dominated groups (Reber et al. 2008; Goumans & Bromley 2013).

Beside these bands, the spectrum displays peaks that are not found in the commercial silicon monoxide compound, which was measured for comparison. The peaks at 2248 and 3327 cm⁻¹ are attributed to the stretching vibrations of SiH and OH groups, respectively. These groups were possibly formed in the condensation or by reaction of the freshly-condensed SiO grains with residual

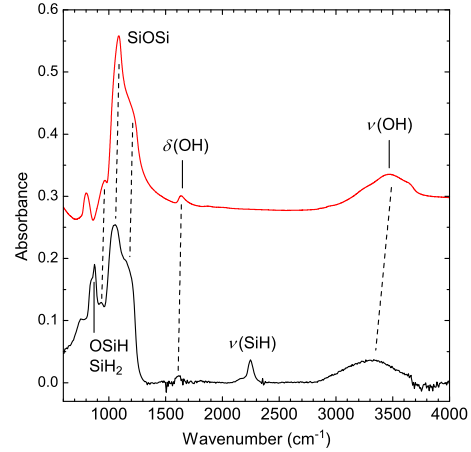


Fig. 3.— Infrared spectrum of a single 20 μm particle collected after the annealing and evaporation of a Ne matrix doped with SiO molecules and oligomers (lower curve, black) in comparison to a SiO₂ material produced by the sol gel technique (upper curve, red). (A color version of this figure is available in the online journal.)

H₂O molecules during the warming to room temperature in the vacuum chamber. However, the OH groups can also be due to water molecules adsorbed on the surface of the grains and of the KBr substrate. The formation of silanol groups (Si–OH) either on the surface or within the silicate structure during the condensation and the warm up of the substrate is very likely. The presence of a small Si–OH stretching band at 932 cm⁻¹ confirms this assumption.

The OH stretching bands of single, paired, and hydrogen-bonded silanol groups are expected between 3750 and 3540 cm⁻¹ (Tyler et al. 1969; Armistead et al. 1969). Due to the presence of water vapor lines near 3800 cm⁻¹, it is difficult to ascertain the presence of a band corresponding to OH stretching modes of such silanol groups. The broad band at 3327 cm⁻¹ that can tentatively be assigned to stretching vibrations of interacting water molecules and silanol groups (Si–OH) (Zhdanov et al. 1987) supports the existence of these groups. However, a firm discrimination between water molecules either adsorbed on the surface of the grains or on the KBr is difficult. The weak band at 1614 cm⁻¹ is attributed to the corresponding bending mode

$\delta(\text{OH})$ of water molecules whereas bands at 843 and 873 cm^{-1} can be assigned either to vibrations of O-SiH groups (Shinoda et al. 2006) or to vibrations of Si-Si bonds of the sesquioxide group Si_2O_3 (Day & Donn 1978; Hagenmayer et al. 1998). A similar band was already observed in amorphous silicates of olivine and pyroxene stoichiometry produced by condensation in a H_2O containing atmosphere at high temperatures (Jäger et al. 2009). Our experiments have shown that Si-H bonds can easily be destroyed by oxygen or oxygen-bearing molecules. In the dense ISM, where a lot of oxygen-bearing molecules such as H_2O , CO, CO_2 , and many other species plate out on the surface of the cold grains, reactions between Si-H bonds and these molecules may occur resulting in the formation of Si-O bonds. Of course, we do not exactly know the energy barriers for these reactions, but cosmic rays may help to speed up the processes. In less dense regions of molecular clouds and in diffuse cold clouds, the substitution of H can be enhanced by UV irradiation. All things considered, the IR spectral measurements of the condensate clearly show the formation of a solid SiO_x compound that reveals the spectral signatures of SiO_2 .

3.2. Helium Droplet Isolation Studies

To study the condensation of silicon oxide grains inside helium droplets, we apply two different approaches. We study the co-condensation of water molecules together with Si atoms and together with SiO molecules. Both routes should be relevant to the processes occurring in the ISM. Depending on the conditions for the destruction of the stellar silicate grains, the formation of SiO molecules or Si atoms is expected. Additionally, Si and SiO species may arrive to the ISM directly from the stellar regions, and SiO molecules can be formed in the reaction $\text{Si} + (\text{O}_2, \text{OH})$ (Turner 1998). At the same time, the water molecule is the most abundant oxygen-bearing molecule in the Universe and could serve as an oxidizer for Si and SiO species, which are accreted on the surface of dust particles.

3.2.1. Initial Cluster Formation

The initial stage of cluster formation was studied by the means of quadrupole mass spectrometry. The mass spectra were obtained after electron

impact ionization of the doped helium droplets. The ionization of a helium droplet results in the formation of He^+ . This positive charge migrates through the droplet via a positive-hole resonant-hopping mechanism. In the case of relatively small helium droplets with less than 30 000 helium atoms, the migration process terminates when the charge is transferred from He^+ to the dopant or when the charge becomes localized at another helium atom to create He_n^+ (Scheidemann et al. 1993). The excess energy ejects the ionized dopant or the He_n^+ cluster from the droplet. As a result, the dopant and helium cluster cations are observed as fragments of the helium droplets in the mass spectrum on their respective masses. Unfortunately, with the increase of the helium droplet size, the probability of charge transfer to the dopant is reduced and only He_n peaks can be detected by mass spectrometry. Therefore, mass spectrometry combined with electron impact ionization cannot be applied to study the formation of large clusters as their assembly requires much larger helium droplets containing a few millions of helium atoms.

Figure 4(a) shows the mass spectrum of helium droplets doped with silicon atoms and water molecules. Compounds with the formula $\text{Si}_x\text{O}_y\text{H}_z$ ($x = 1-2$, $y = 1-3$, and $z = 0-3$) can be identified. Although it is not shown with this figure, the peak intensities of products with larger y and z grow as the water concentration increases. As it was previously found that Si atoms and small clusters do not form chemical bonds with H_2O molecules inside He droplets (Krasnokutski & Huisken 2010a), these compounds were formed by ion-molecule reactions after charge transfer from He^+ to the $\text{Si}_x(\text{H}_2\text{O})_y$ complexes.

Figure 4(b) depicts the mass spectrum measured when the He droplets are doped with SiO and H_2O molecules. This mass spectrum was obtained with the lower-resolution mode of the mass spectrometer, which allows to access a considerably higher mass range. Mass peaks corresponding to various Si_xO_y clusters can be observed, including $(\text{SiO})_k$ clusters indicated with values of k . The observation of $(\text{SiO})_k$ clusters formed in He droplets is consistent with the results of our matrix isolation study (see Section 3.1) and with literature data (see Introduction). We suppose that the presence of species with higher oxygen content ($y > x$) reveals ion-molecule reactions be-

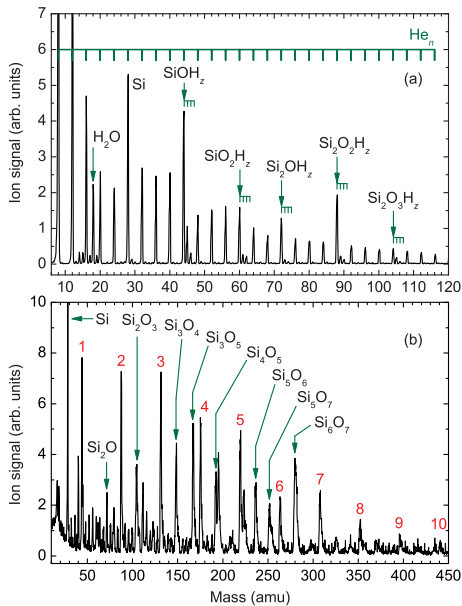


Fig. 4.— Mass spectra of He droplets doped with Si atoms and H₂O molecules (a) and with SiO and H₂O molecules (b). In panel (a), Si_xO_yH_z compounds are indicated with (green) arrows. The small scales beneath the arrowheads mark the different values of z ($z = 0-3$). In panel (b), the Si_xO_yH_z compounds with $z > 0$ are not resolved, therefore they are not indicated. The mass peaks corresponding to (SiO) _{k} clusters are labelled (in red) with values of the natural number k . (A color version of this figure is available in the online journal.)

tween SiO and H₂O species rather than the loss of Si atoms upon ionization. The low resolution of the spectrum does not allow us to clearly separate the Si_xO_yH_z from the Si_xO_y species, however, the presence of such cations is firmly determined. Specific mass peaks exhibit much higher intensities than other peaks in the same mass range. The large intensity of these mass peaks reflects the high stability of the corresponding cations and reveals a considerable fragmentation caused by the ionization or the reactions triggered by the ionization process.

To study the reactions of SiO molecules inside the droplets before the ionization point, we applied the calorimetric approach. In the case of a chemical reaction, the energy released during the reaction is transferred to the He droplet, causing

the evaporation of He atoms. The change of the He droplet size upon reaction can be detected in the experiment. This calorimetric technique was already applied to study chemical reactions inside helium droplets (Krasnokutski & Huisken 2010a, 2011). Another calorimetric method recently developed by Lewis et al. (2012) is well suited to the study of cluster formation. The idea behind this technique is the determination of the smallest helium droplet size that allows the assembly of the desired cluster inside the droplet. If the helium droplet is smaller than this minimum size it would be completely destroyed upon the reaction and it would not arrive at the detector. As a result, during a continuous increase of the helium droplet size by varying the droplet source temperature, a distinct rise of the number of (SiO) _{k} cations occurs when the helium droplet becomes larger than the minimum size required for the dissipation of the binding energy of this (SiO) _{k} cluster. We have applied the basic principle of this technique, with a development of our own, to monitor the formation of SiO clusters. The detailed description of the procedure is given in Appendix A.

The reaction energies we have determined experimentally are summarized in Table 1 together with the values obtained from quantum chemical calculations. All computational values presented in the table were derived assuming cyclic reaction products. They are consistent with our experimentally derived values for binding energies that confirm the formation of cyclic products by barrierless reactions. This is in agreement with the results of previous IR spectroscopy studies of cryogenic matrices (Anderson et al. 1968; Hastie et al. 1969; Anderson & Ogden 1969). However, Friesen et al. (1999) did not observe barrierless reactions for the SiO oligomerization in methane cryogenic matrices. Moreover, Pimentel et al. (2006) determined an energy barrier of 8 kcal mol⁻¹ for the reaction between Si₂O₂ and SiO.

At the current state, it is difficult to accurately calculate the error for the experimental determination of the reaction enthalpy within the helium droplets since a few simplifications were used in the analysis. In Appendix A, a more detailed discussion of the error is performed and it is estimated to be smaller than 30%. Therefore, the difference between the present computational and

Table 1: Reaction Energies

Reaction	Energy				
	Observed	Theoretical			
		Model 1 ^a	Model 2 ^b	Model 3 ^c	Model 4 ^d
SiO + SiO → Si ₂ O ₂	178	170	211	201	163
Si ₂ O ₂ + SiO → Si ₃ O ₃	291	248	240	241	253
(SiO + SiO) + H ₂ O → Si ₂ O ₂ OH ₂	206	172			
(Si ₂ O ₂ + SiO) + H ₂ O → Si ₃ O ₃ OH ₂	249	244			

^aB3LYP/6-311+G**, this work.

^bCCSD(T)/cc-pVTZ, this work.

^cB3LYP/6-31G** (Friesen et al. 1999).

^dQCISD/6-311++G** (Pimentel et al. 2006). The original values were expressed in units of kcal mol⁻¹.

NOTE.—Reaction energies are expressed in units of kJ mol⁻¹.

experimental values is within the uncertainty interval of the measurements and thus suggests that these reactions indeed took place inside the helium droplets at $T = 0.37$ K and led to the formation of cyclic (SiO)_k clusters. This demonstrates that the formation of cyclic (SiO)_k clusters is barrierless and should be fast in the entire low-temperature range and its reaction rate is defined by the collision probabilities of the SiO molecules. The absence of an energy barrier for the insertion of the SiO molecule into the Si₂O₂ ring with four equally strong Si-O bonds demonstrates that the existing Si-O bonds can easily rearrange into energetically favored structures. Although Si_xO_y compounds linked to the presence of H₂O were observed in the experiments, we suppose that they were formed by the ionization process.

3.2.2. Grain Formation

To produce solid material inside the droplets, the nozzle temperature was reduced to $T = 8$ K resulting in He droplets containing about 10⁷ He atoms. The vapor pressure of the dopants was kept the same as in the previous experiments. Nevertheless, the 40-times increase of the geometrical cross section of the He droplets also resulted in an increase of the number of dopants picked up. To collect the condensate formed in the droplets, a lacey carbon TEM grid was inserted into the beam of the doped helium droplets. The deposit on this grid was analyzed by HRTEM and EDX. Figure 5 shows HRTEM images of the deposit ob-

tained with helium droplets doped with Si atoms and H₂O molecules (1. experiment) [Figures 5(a) and 5(b)] and with SiO, O₂, and H₂O molecules (4. experiment) [Figures 5(c) and 5(d)]. In both cases, we observe large silicon oxide grains, which cannot be produced inside single helium droplets. This demonstrates that additional aggregation of the nanometer-sized condensates takes place on the substrate.

The TEM image in Figure 5(a) shows numerous dark spots inside a grain produced by doping helium droplets with Si and H₂O. The EDX analysis of these spots has demonstrated their chemical identity with the main body of the particle, pointing to a thickness contrast, exclusively. Therefore, these spots likely represent particles grown in individual He droplets. Additional support for this interpretation is provided by the fact that the size of these smaller particles is about 10 nm [see Figure 5(b)], which is also the size of the silver nanoparticles grown in helium droplets under similar experimental conditions (Loginov et al. 2011b).

The analysis of the TEM image in Figure 5(c) yields a similar conclusion concerning condensation experiments with SiO and H₂O/oxygen. The slowly decreasing SiO vapor pressure, however, leads to the formation of smaller particles in the helium droplets, with an average size of 3 nm, as shown in Figure 5(d). The EDX analysis revealed the formation of SiO₂ grains that supports the concept of a condensation within the He clusters

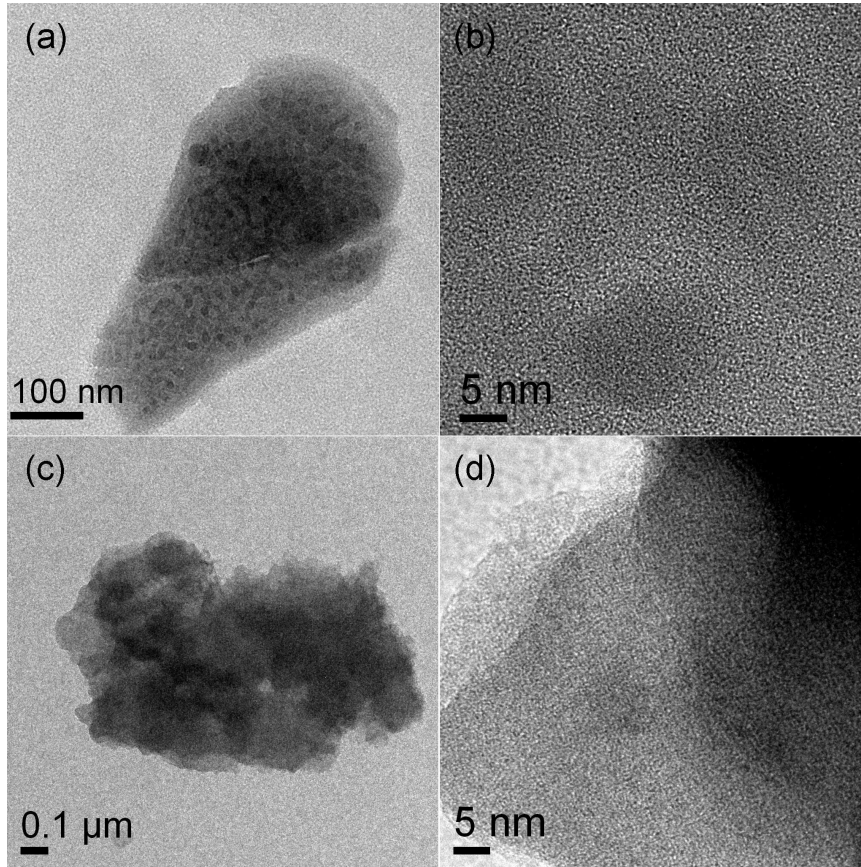


Fig. 5.— TEM images showing the particles formed on the substrate placed in the He droplet beam when the droplets were doped with Si atoms and H₂O molecules [(a) and (b)], and with SiO and H₂O molecules [(c) and (d)].

since a later oxidation of SiO grains with oxygen molecules at room temperature is found to be very slow (Fogarassy et al. 1987).

4. ASTROPHYSICAL DISCUSSION

In our experiments, we have observed the formation of silicon oxide grains at low temperature. In the matrix isolation experiment, the SiO grains were formed by reaction between SiO molecules during the annealing (10–11 K) and evaporation of the Ne matrix (12 K), that is under conditions comparable to those expected in molecular clouds. The study of different dopant molecules (Si and H₂O; SiO; SiO and H₂O; SiO, H₂O, and O₂) in superfluid He droplets has shown that the reaction between SiO molecules can take place already at 0.37 K and is therefore barrierless. Consequently,

the condensation of solids should be as well possible at higher temperatures (10–300 K). Furthermore, the results have shown that Si atoms can be easily oxidized.

Certainly, solid SiO is not considered as an abundant cosmic dust component. Pure SiO_x grains are not observed in the ISM while the presence of Mg-Fe silicates has been proven (Henning 2010). However, gaseous SiO is one of the main precursors for silicates in evolved stars (Gail & Sedlmayr 1999).

In the ISM, SiO can be produced by different ways, such as photodesorption of SiO from silicate grains by UV irradiation (Turner 1998), and sputtering of Si followed by the oxydation to SiO molecules in shock waves (Gusdorf et al. 2008a,b). SiO emissions in molecular clouds be-

cause of shock waves have also been observed (Dishoek 1993; Martin et al. 1997; Handa et al. 2006; Nguÿên-Lu'o'ng et al. 2013). Recently, the formation of pure SiO grains in the shells of S-stars has been proposed (Wetzell et al. 2013). The study of the formation of SiO condensates at low temperatures is the first step into the direction of the more complex magnesium-iron silicates of olivine and pyroxene stoichiometry.

The dust condensation at low temperature and low density in the ISM is a process that is discussed to be necessary to keep the balance between dust destruction and formation (Chiaki et al. 2013). However, there is no exact description where the cold condensation process may finally take place. Dust can be easily destroyed in SN shocks. Turbulence can quickly distribute the delivered refractory elements such as Mg, Si, and other species into the surrounding ISM. Oey (2003) estimated that freshly synthesized metals from SN ejecta are mixed by turbulence with the surrounding ISM on a time scale of 100 Myr. One can assume a similar time scale for the mixing of elements liberated from destroyed grains.

The process of cold condensation may already be active in diffuse clouds with low temperature and in low-density regions of molecular clouds. In molecular cloud environments with maximum density, where many non-refractory and refractory species and elements may accrete simultaneously on the grains, rather complex ices are formed and the formation of silicates and other solids could be restricted. However, dust grain formation is essentially a process which can be described by two steps: nucleation and growth. If the elements which are heavily depleted in the ISM stick efficiently to the surviving grains, then, accretion onto grains occurs quickly enough to account for their depletion. A previous nucleation step is not necessary to form solids. If refractory atoms and molecules accrete slowly onto the surfaces of surviving grains, such atoms have the opportunity to react with additional adsorbed atomic and molecular species before being buried beneath a growing layer. The most abundant atomic species is H and the most abundant molecules are H₂, CO, and H₂O. Therefore, reactions between refractory elements and these molecules might also form complex ices. There are two competitive processes af-

fecting the growth of the layer which is the desorption of molecules due to irradiation and the sticking. While the sticking of an atom or molecule to a grain is a process of low selectivity at low temperatures, the desorption process is strongly influenced by the bonding energy between the atom or molecule and the surface. According to Draine (2009), for binding energies of 0.05 eV, the lifetime against thermal desorption is about 1 s, whereas for a binding energy of 0.1 eV, the lifetime is increased to a value of 5×10^5 yr. Molecules or atoms that may form strong bonds, which are typical for refractory solids, grow very fast and remain on the surface for a long time. Moreover, diffusion/desorption processes on grain surfaces may occur, and eventually, lead to the formation of stable solids such as silicates or carbonaceous material in addition to complex ices. Such possible selection processes have to be addressed in upcoming experimental studies.

In addition, our experiments have shown that SiO can form clusters that can finally condense as solid silicon oxide. Since these reactions occur without an energy barrier, no further irradiation with UV or cosmic-ray energy protons is necessary to form solids. Barrierless structural rearrangements in SiO clusters are possible. This has been demonstrated by quantum chemical computations that show the tendency of SiO clusters to disproportionate into SiO₂ and Si phases (Reber et al. 2008; Goumans & Bromley 2013, Bromley priv. communication). UV irradiation may help to rearrange the bonds in the SiO clusters. Furthermore, UV irradiation can help to desorb non-refractive species that form complex ices and prevent the formation of solids. Moreover, all gaseous species should be depleted on grains within a timescale of 1×10^5 yr in dense clouds. Since these clouds have longer lifetimes of about 10 Myr and some species are still observed in the gas phase, there must be a mechanism to frequently remove the mantles of accreted species from the grain surfaces. Such mechanisms should result in the preferred formation of compounds with higher binding energy such as silicates and should remove the weakly bound species in ice mantles.

In general, dense molecular clouds are not completely protected from the interstellar UV field since diffuse UV photons from outside and from

newly born stars inside the clouds can deeply penetrate even the interior of such a cloud. In addition, cosmic rays can penetrate the molecular clouds and similarly trigger reactions between accreted molecules and clusters. Previous studies of reactions in He clusters showed that Si, Mg, and Al atoms also reacted with O₂ molecules at very low temperatures (Krasnokutski & Huisken 2010a,b, 2011). Of course, the fact that there is no energy barrier at the entrance channel of a reaction between two atoms or molecules does not mean that its product can be finally formed in the gas phase in the ISM. Actually, the excess energy generated by the reaction can cause the dissociation of the product if it cannot be released by another means like the emission of photons. When a species reacts with the surface of a preexisting grain, however, the excess energy can be transferred to this grain, which plays the role of a heat sink.

In the ISM, UV irradiation with 10 eV photons and low-energy ion irradiation due to acceleration of ions and atoms in shock waves can strongly force the formation of solids. However, polymerization and photodesorption of molecules are competitive processes. Chemical reactions between adsorbed molecules and the grain surface can prevent the desorption of the adsorbate. In the grains condensed at low temperatures, the defect formation is a very probable process since the diffusion of atoms within the structure of the solids is strongly slowed down preventing the annealing of possible defects. In addition, IR spectroscopy of the condensed grains clearly show the appearance of IR bands at 873 and 2248 cm⁻¹ which point to the presence of Si–H bonds or special structures related to the sesquioxide group Si₂O₃. These bands appear in addition to the two typical bands caused by Si–O bonds in silicon oxides or in silicates. Si–Si or Si–H bonds that can be easily destroyed upon UV or ion irradiation can finally act as such defects and may change the sticking behavior of the molecules on the grain surface.

Experimental studies on the carbon dust formation in the ISM performed by Jenniskens et al. (1993) have shown the formation of carbon dust upon UV and ion irradiation. The authors found that dust particles accrete a layer of about 20 nm during their lifetime in a molecular cloud. UV photons clearly dominate the polymerization and

carbonization process even though the process is much more efficient for ion-induced polymerization.

The SiO grains formed by low temperature condensation have an irregular, fluffy morphology. In that respect they do not differ from grains condensed at relatively higher temperatures (Colangeli et al. 2003). Their structure is amorphous and therefore very well comparable to the structure of the observed interstellar silicates. The degree of crystallinity for interstellar silicates was determined not to be higher than 2.2% (Kemper et al. 2004, 2005; Min et al. 2007).

Future experiments on dust formation in the ISM including SiO and refractory elements such as Mg and Fe in cryogenic matrices and on bare surfaces are in progress. In situ IR spectroscopy of the condensed layers during the growth process is necessary to follow the formation of bonds and defects and the effect of annealing in the structure of the condensate.

5. CONCLUSION

The condensation of silicon monoxide at low temperature was studied in solid neon matrices and superfluid helium droplets. The initial stage of condensation was investigated in the helium droplets by mass spectrometry and by quantum chemical calculations. The formation of cyclic (SiO)_k ($k = 2-3$) clusters inside helium droplets at $T = 0.37$ K has been found to be barrierless. The binding energies of (SiO)_k ($k = 2-3$) clusters were obtained by measuring the minimum size of helium droplets that is necessary for assembling the desired cluster. Additionally, the formation of nanometer to micrometer-sized silica grains was observed after evaporation of the liquid helium droplets or the neon matrix doped by single SiO molecules. These results clearly demonstrate the formation of solid SiO at low temperature, which is an important requirement for the formation of more complex silicates in the entire low temperature range of the ISM. The analysis of the particles reveals an amorphous structure with a high surface area. Thus it appears necessary to consider cosmic dust analogs formed at low temperatures when interpreting astrophysical observations. The data presented in this article demonstrate the power of the matrix and helium droplet isolation tech-

niques to study low temperature dust formation. The extension of this study to silicates with different Mg and Fe contents and with in situ spectral characterization of the dust grains formed in the experiments, is planned.

This work was supported by the Deutsche Forschungsgemeinschaft, DFG project number He 1935/26-1, which is a part of the DFG priority program 1573 'Physical Processes in the ISM'. We are grateful to Frank Hänschke, IPHT Jena, for performing the FTIR microscope measurement. We are also grateful to J. Nuth for his helpful discussions.

REFERENCES

- Anderson, J. S., & Ogden, J. S. 1969, *J. Chem. Phys.*, 51, 4189
- Anderson, J. S., Ogden, J. S., & Ricks, M. J. 1968, *Chem. Commun. (London)*, 1968, 1585
- Andrews, L. 2004, *Chem. Soc. Rev.*, 33, 123
- Armistead, C. G., Tyler, A. J., Hambleton, F. H., Mitchell, S. A., & Hockey, J. A. 1969, *J. Phys. Chem.*, 73, 3947
- Avramov, P. V., Adamovic, I., Ho, K.-M., et al. 2005, *J. Phys. Chem. A*, 109, 6294
- Barlow, M. J., & Silk, J. 1977, *ApJ*, 211, L83
- Chiaki, G., Nozawa, T., & Yoshida, N. (2013) *ApJ*765, L3
- Chin, S. A., & Krotscheck, E. 1995, *Phys. Rev. B*, 52, 10405
- Colangeli, L., Henning, Th., Brucato, J. R., et al. 2003, *A&AR*, 11, 97
- Day, K. L., & Donn, B. 1978, *Science*, 202, 307
- Delley, B. 2006, *J. Phys. Chem. A*, 110, 13632
- van Dishoeck, E., Jansen, D.J., & Phillips, T. G. 1993, *A&A*, 279, 541
- Donn, B., Hecht, J., Khanna, R., et al. 1981, *Surf. Sci.*, 106, 576
- Draine, B. T. 2009, in *ASP Conf. Ser. 414, Cosmic Dust – Near and Far*, ed. Th. Henning, E. Grün, & J. Steinacker (San Francisco, CA: ASP), 453
- Draine, B. T., & Salpeter, E. E. 1979, *ApJ*, 231, 438
- Dwek, E., & Scalo, J. M. 1980, *ApJ*, 239, 193
- Ferguson, F. T., & Nuth, J. A. 2012, *J. Chem. Eng. Data*, 57, 721
- Fogarassy, E., Slaoui, A., Fuchs, C. & Regolini, J. L. 1987, *Appl. Phys. Lett.* 51, 337
- Friesen, M., Junker, M., Zumbusch, A., & Schnöckel, H. 1999, *J. Chem. Phys.*, 111, 7881
- Frisch, M. J., Trucks, G. W., Schlegel, H. B., et al. 2009, *Gaussian 09, Revision A.02* (Wallingford CT: Gaussian, Inc.)
- Gail, H.-P., & Sedlmayr, E. 1999, *A&A*, 347, 594
- Goumans, T. P. M., & Bromley, S. T. 2013 *Phil. Trans. R. Soc. A*, 371, 20110580
- Gusdorf, A., Cabrit, S., & Flower, D. R., & Pineau des Forts, G. 2008 *A&A*482, 809
- Gusdorf, A., Pineau des Forts, G., Cabrit, S., & Flower, D. R. 2008 *A&A*490, 695
- Hagenmayer, R. M., Friede, B., & Jansen, M. 1998, *J. Non-Cryst. Solids*, 226, 225
- Handa, T., Sakano, M., Naito, S., Hiramatsu, M., & Tsuboi, M. 2006, *Journal of Physics: Conference Series* 54, 47
- Hartmann, M., Miller, R. E., Toennies, J. P., & Vilesov, A. F. 1996a, *Science*, 272, 1631
- Hartmann, M., Toennies, J. P., Vilesov, A. F., & Benedek, G. 1996b, *Czechoslovak J. Phys.*, 46, 2951
- Hastie, J. W., Hauge, R. H., & Margrave, J. L. 1969, *Inorg. Chim. Acta*, 3, 601
- Henning, Th. 2010, *ARA&A*, 48, 21
- Herbst, E. 2001, *Chem. Soc. Rev.*, 30, 168
- Hormes, J., Sauer, M., & Scullman, R. 1983, *J. Mol. Spectrosc.*, 98, 1
- Hohl, A., Wieder, T., van Aken, P. A., Weirich, T. E., Denninger, G., Vidal, M., Oswald, S., Deneke, C., Mayer, J., Fuess, H. 2003, *J. Non-Cryst. Sol.*, 320, 255

- Jacox, M. E. 2002, *Chem. Soc. Rev.*, 31, 108
- Jäger, C., Mutschke, H., Henning, T. & Huisken, F. in *ASP Conf. Ser.* 414, *Cosmic Dust – Near and Far*, ed. Th. Henning, E. Grün, & J. Steinacker (San Francisco, CA: ASP), 319
- Jenniskens, P., Baratta, G. A., Kouchi, A., et al. 1993, *A&A*, 273, 583
- Jones, A. P., Tielens, A. G. G. M., Hollenbach, D. J., & McKee, C. F. 1994, *ApJ*, 433, 797
- Jones, A. P., & Nuth, J. A. 2010, *A&A*, 530, A44
- Kemper, F., Vriend, W. J., & Tielens, A. G. G. M. 2004, *ApJ*, 609, 826
- Kemper, F., Vriend, W. J., & Tielens, A. G. G. M. 2005, *ApJ*, 633, 534
- Khanna, R. K., Stranz, D. D., & Donn, B. 1981, *J. Chem. Phys.*, 74, 2108
- Krasnokutski, S., Rouillé, G., & Huisken, F. 2005, *Chem. Phys. Lett.*, 406, 386
- Krasnokutski, S. A., & Huisken, F. 2010a, *J. Phys. Chem. A*, 114, 13045
- Krasnokutski, S. A., & Huisken, F. 2010b, *J. Phys. Chem. A*, 114, 7292
- Krasnokutski, S. A., & Huisken, F. 2011, *J. Phys. Chem. A*, 115, 7120
- Lewerenz, M., Schilling, B., & Toennies, J. P. 1995, *J. Chem. Phys.*, 102, 8191
- Lewerenz, M., Schilling, B., & Toennies, J. P. 1997, *J. Chem. Phys.*, 106, 5787
- Lewis, W. K., Harruff-Miller, B. A., Gord, M. A., et al. 2012, *Rev. Sci. Instrum.*, 83, 073109
- Loginov, E., Gomez, L. F., Chiang, N., et al. 2011a, *Phys. Rev. Lett.*, 106, 233401
- Loginov, E., Gomez, L. F., & Vilesov, A. F. 2011b, *J. Phys. Chem. A*, 115, 7199
- Lu, W. C., Wang, C. Z., & Ho, K. M. 2003, *Chem. Phys. Lett.*, 378, 225
- Min, M., Waters, L. B. F. M., de Koter, A., et al. 2007, *A&A*, 462, 667
- Martin-Pintado, J., De Vicente P., Fuente, A., & Planesas, P. 1997 *ApJ*, 482, L45
- Nguÿên-Lu'ò'ng, Q., Motte, F., Carlhoff, P., Louvet, F., Lesaffre, P., Schilke, P., Hill, T., Hennemann, M., Gusdorf, A., Didelon, P., Schneider, N., Bontemps, S., Duarte-Cabral, A., Menten, K. M., Martin, P. G., Wyrowski, F., Bendo, G., Roussel, H., Bernard, J.-P., Bronfman, L., Henning, T., Kramer, C., & Heitsch, F. 2013 *ApJ*, 755, 88
- Nuth, J. A., & Moore, M. H. 1989, *Proc. Lunar Planet. Sci. Conf.*, 19, 565
- Oey, M. S. 2003, in *Proc. of the IAU Symposium 212, A Massive Star Odyssey: From Main Sequence to Supernova*, ed. K.A. van der Hucht, A. Herrero, & C. Esteban, 620
- Pimentel, A. S., Lima, F. C. A., & da Silva, A. B. F. 2006, *J. Phys. Chem. A*, 110, 13221
- Reber, A. C., Paranthaman, S., Clayborne, P. A., Khanna, S. N., & Castleman, A. W. 2008, *ACS Nano*, 2, 1729
- Rouillé, G., Steglich, M., Carpentier, Y., et al. 2012, *ApJ*, 752, 25
- Ruchti, T., Förde, K., Callicoatt, B. E., Ludwigs, H., & Janda, K. C. 1998, *J. Chem. Phys.*, 109, 10679
- Scheidemann, A., Schilling, B., & Toennies, J. P. 1993, *J. Phys. Chem.*, 97, 2128
- Schnöckel, H., Mehner, T., Plitt, H. S., & Schunck, S. 1989, *J. Am. Chem. Soc.*, 111, 4578
- Shinoda, K., Yanagisawa, S., Sato, K., & Hirakuri, K. 2006, *J. Crystal Growth*, 288, 84
- Shirk, J. S., & Bass, A. M. 1968, *J. Chem. Phys.*, 49, 5156
- Toennies, J. P., & Vilesov, A. F. 2004, *Angew. Chem. Int. Ed.*, 43, 2622
- Turner, B. E. 1998, *ApJ*, 495, 804
- Tyler, A. J., Hambleton, F. H., & Hockey, J. A. 1969, *J. Catal.*, 13, 35
- Vongehr, S., Chun, T. S., & Kang, M. X. 2010, *Chinese Phys. B*, 19, 023602

- Walmsley, C. M., Pineau des Forêts, G., & Flower, D. R. 1999, A&A, 342,542
- Weingartner, J. C., & Draine, B. T. 1999, ApJ, 517, 292
- Wetzel, S., Klevenz, M., Gail, H.-P., Pucci, A., & Trieloff, M. 2013, A&A, 553, A92
- Xu, G. L., Liu, X. F., Xie, H. X., Zhang, X. Z., & Liu, Y. F. 2010, Chinese Phys. B, 19, 113101
- Zhdanov, S. P., Kosheleva, L. S., & Titova, T. I. 1987, Langmuir, 3, 960
- Zhukovska, S., Gail, H.-P., & Trieloff, M. 2008, A&A, 479, 453

A. EVALUATION OF REACTION ENERGIES

In our He droplet experiment, the vapor pressure of SiO was kept constant and the number of cations at specific masses was counted as a function of the helium droplet size. We monitored the ion count rate at the masses of $(\text{SiO})_k$ clusters and their complexes with water molecules $(\text{SiO})_k\text{OH}_2$. In the latter case, we set the vapor pressure of water so as to achieve a probability of doping the helium droplets with H_2O molecules close to 100%. As a result, the signal at the mass of any $(\text{SiO})_k\text{OH}_2$ compound is defined by the number of helium droplets containing the corresponding $(\text{SiO})_k$ cluster. Monitoring the $(\text{SiO})_k\text{OH}_2$ signal has the advantage that the mass of such a compound does not coincide with the mass of a He_n cluster, unlike that of a $(\text{SiO})_k$ cluster. Additionally, these complexes can be formed only inside the He droplets.

Ion count rates as a function of the helium droplet size are shown in Figure 6(a). They increase with the size of the helium droplets, reflecting the fact that larger droplets pick up more molecules and they are more efficiently ionized. The onset of the ion signal rise for increasing $(\text{SiO})_k$ cluster sizes is shifted towards bigger helium droplets revealing the larger amount of energy released in the oligomerization processes. In contrast with previous studies by Lewis et al. (2012), our ion signals do not show sharp thresholds. Their intensities rise rather smoothly towards larger helium droplet sizes. This observation can be understood taking into account that the sizes of the He droplets follow a log-normal distribution. To find the minimum helium droplet size required for the $(\text{SiO})_k$ cluster formation, we compared the experimentally derived numbers of $(\text{SiO})_k$ ions with the calculated probability of $(\text{SiO})_k$ ion formation P that can be calculated with

$$P = P_k P_1 P_{CT}, \quad (\text{A1})$$

where P_k is the probability for a helium droplet to pick up k SiO molecules, P_1 is the probability to ionize a droplet, and P_{CT} represents the probability for the charge transfer from the droplet to its dopant. When the partial evaporation of the droplet, that occurs at each pick up event, can be neglected, the probability P_k can be estimated by a Poisson distribution (Lewerenz et al. 1995, 1997). Since we want to determine the

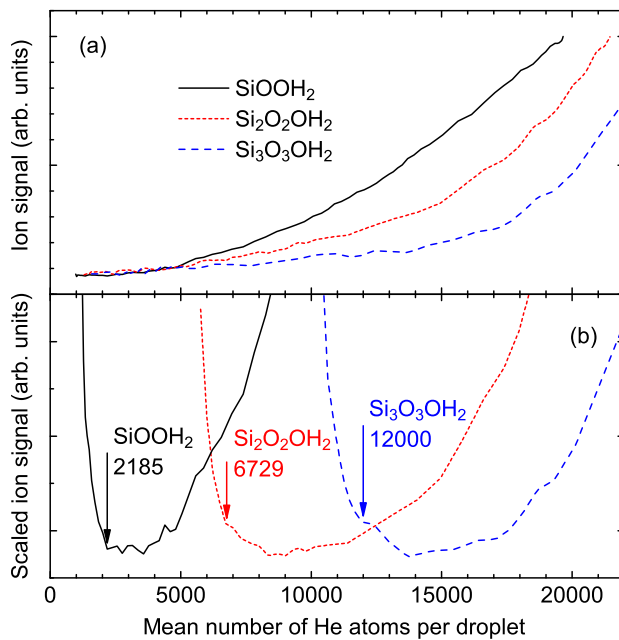


Fig. 6.— Mass spectrometry signal of various cations as a function of the average number of He atoms per droplet. Panel (a) shows the raw measurements. The data depicted in panel (b) have been derived by scaling the data of panel (a). (A color version of this figure is available in the online journal.)

smallest droplet size for which the assembly of a given product is possible, the evaporation of the droplet is a critical parameter and the Poisson distribution is no longer valid.

We regard the probability to pick up k SiO molecules as a product of the probabilities of single collision events multiplied by the probability of not picking up additional molecules. This is given by

$$P_k = \exp(-n_{\text{SiO}}\sigma_k l_k) \prod_{i=0}^{k-1} [1 - \exp(-n_{\text{SiO}}\sigma_i l_i)], \quad (\text{A2})$$

where n_{SiO} is the number density of SiO molecules in the pick-up region, σ_i the pick-up (geometrical) cross section of the droplet after picking up i SiO molecules, and l_i the rest length of the pick-up region. This approach will be discussed in more detail in a forthcoming paper.

Similarly, the probability for a helium droplet to collide with an electron in the ionizer can be expressed by

$$P_1 = 1 - \exp(-n_{\text{el}}\sigma_k l_{\text{ion}}), \quad (\text{A3})$$

where n_{el} is equal to the number density of electrons in the ionization region of the length l_{ion} . The parameters n_{SiO} and n_{el} are determined by the conditions of the experiment such as the temperature of the oven used to produce SiO molecules and the current of the ionizer.

Finally, using the experimental data from Ruchti et al. (1998), we conclude that the probability for charge transfer can be described by a decreasing linear function on the number of He atoms in the droplet. Hence,

$$P_{\text{CT}} = 1 - cN_k. \quad (\text{A4})$$

Initially, the parameter c was set to achieve a probability of 50% for the charge transfer in the largest helium droplets used in our experiment. Moreover, we neglected the change of the helium droplet size upon pick-up of SiO molecules. After a first evaluation of the reaction energies (see below), we used the σ_i values determined by the experiment in Equation A2 and repeated the analysis. This procedure was repeated until the derived binding energies did not change anymore. It was also found that the variation of the parameter c , which results in a change of the charge transfer probability in the largest helium droplets from 10% to 100%, does not affect the values of the reaction energies.

In this analysis, several approximations were used. We did not consider the scattering of the helium droplet beam and the non-symmetrical size distribution of the helium droplets. Moreover, the velocity distributions of the SiO molecules and electrons was not taken into account. All this is expected to cause some inaccuracy of the calculated ion signal P . The effect of such simplifications was already analyzed in a former paper and the error was amounted to be up to 30% for the evaluation of the ion signals (Vongehr et al. 2010). However, when the helium droplet is below its minimum size required for the assembly of the desired cluster, the difference between the measured and calculated ion signal should be extremely large. Therefore, a simple modeling of the ion signal dependence on the He droplet size allows us to accurately identify the point where the experimental values start to deviate from the calculated behavior. As a result, we expect that such a procedure can provide an accuracy much better than 30% for the evaluation of the reaction energies. To compare the theoretical and experimental values, we have scaled the experimentally measured ion intensities by dividing by the probability P (see Equation A1).

The experimental determination of reaction energies relies on studies of He droplets, which were the subject of numerous publications. Temperatures, sizes, and size distributions of He droplets are well known (Toennies & Vilesov 2004). Excited molecules inside He droplets relax to the ground state in a sub-nanosecond time scale transferring their energy to the liquid helium, which is the basis of our experimental analysis. The only other way to dissipate the energy is a non-thermal ejection of reaction products or photon emission. Non-thermally ejected reaction products cannot be detected by mass spectrometry. The reason is the much smaller ionization cross section compared with the ionization cross section of He droplets. Our system does not detect these products and therefore, they do not contribute to the determined reaction energy. Photon emission can dissipate a considerable amount of energy resulting in a strong discrepancy

between experimentally and computationally derived values of reaction enthalpy, which is not the case in our analysis.

The scaled intensities [see Figure 6(b)] show regimes with different slopes. In the range of small helium droplets, the capacity of the helium droplets to dissipate the heat of condensation is not sufficient to allow the assembling of the corresponding $(\text{SiO})_k$ cluster. Non-scaled ion signals demonstrate a very slow increase in this size regime [Figure 6(a)], which is mainly due to the size distribution of the helium droplets and the presence of large helium droplets in the beam. However, this increase is very small and, after scaling, we obtain a strong decrease of the ion intensities as a function of the average droplet size [Figure 6(b)]. When the helium droplets reach the minimum size, which is sufficient to assemble a $(\text{SiO})_k$ cluster, we observe a sudden change of the slope of the scaled signals. After this point, the non-scaled ion intensities increase as predicted for a short range and then start to rise. The rise is due to the fact that $(\text{SiO})_k$ ions are produced by fragmentation of larger clusters during the ionization process. This gives an additional rise to the ion signals on the $(\text{SiO})_k$ mass.

To compute the condensation or reaction energies, we assume that the evaporation of a single helium atom removes 5 cm^{-1} equivalent energy from the droplet (Chin & Krotschek 1995). The sizes of helium droplets found from Figure 6 were used to calculate the energy of the $(\text{SiO})_k + \text{SiO}$ reactions. We calculate the difference between the minimum numbers of helium atoms per droplet required to assemble $(\text{SiO})_k$ and $(\text{SiO})_{k+1}$ clusters. An additional energy equivalent to the evaporation of 1100 helium atoms is subtracted, due to the pick-up of the last SiO molecule, with which the $(\text{SiO})_{k+1}$ cluster was formed.